Pharm Res (2013) 30:683–693
DOI 10.1007/s11095-012-0906-2

RESEARCH PAPER

Exploration of Optimal Dosing Regimens of Haloperidol, a D_2 Antagonist, *via* Modeling and Simulation Analysis in a D_2 Receptor Occupancy Study

Hyeong-Seok Lim • Su Jin Kim • Yook-Hwan Noh • Byung Chul Lee • Seok-Joon Jin • Hyun Soo Park • Soohyeon Kim • In-Jin Jang • Sang Eun Kim

Received: 13 June 2012 / Accepted: 10 October 2012 / Published online: 10 November 2012

ABSTRACT

Purpose To evaluate the potential usage of D_2 receptor occupancy (D2RO) measured by positron emission tomography (PET) in antipsychotic development.

Methods In this randomized, parallel group study, eight healthy male volunteers received oral doses of 0.5 (n=3), 1 (n=2), or 3 mg (n=3) of haloperidol once daily for 7 days. PET's were scanned before haloperidol, and on days 8, 12, with serial pharmacokinetic sampling on day 7. Pharmacokinetics and binding potential to D_2 receptor in putamen and caudate nucleus over time were analyzed using NONMEM, and simulations for the profiles of D2RO over time on various regimens of haloperidol were conducted to find the optimal dosing regimens.

Results One compartment model with a saturable binding compartment, and inhibitory E_{max} model in the effect compartment best described the data. Plasma haloperidol concentrations at half-maximal inhibition were 0.791 and 0.650 ng/ml, in putamen and caudate nucleus. Simulation suggested haloperidol 2 mg every 12 h is near the optimal dose.

Conclusion This study showed that sparse D2RO measurements in steady state pharmacodynamic design after multiple dosing could reveal the possibility of treatment effect of D_2 antagonist, and could identify the potential optimal doses for later clinical studies by modeling and simulation.

KEY WORDS biomarker · haloperidol · PET · PK/PD modeling · receptor occupancy

ABBREVIATIONS

BC_{max}	maximum binding capacity
CT	computerized tomography
D_2 receptor	dopamine receptor D_2
EPS	extrapyramidal syndromes
GCP	good clinical practice
ICH	international conference on harmonization guidance
MRI	magnetic resonance imaging
PD	pharmacodynamic
PET	positron emission tomography
PK	pharmacokinetic
K_{assoc}	association rate constant
K_{dissoc}	dissociation rate constant

INTRODUCTION

The process for developing a new drug is expensive, time-consuming, and uncertain with high attrition rates. Much effort is being made to accelerate the process while reducing

H.-S. Lim • Y.-H. Noh • S.-J. Jin
Department of Clinical Pharmacology and Therapeutics
Ulsan University College of Medicine, Asan Medical Center
Pungnap-2-dong
Seoul, Republic of Korea

S. J. Kim • B. C. Lee • H. S. Park • S. E. Kim (✉)
Department of Nuclear Medicine Seoul National University
Bundang Hospital, Seoul National University College of Medicine
300 Gumi-dong, Bundang-gu
Seongnam 463-707, Republic of Korea
e-mail: kse@snu.ac.kr

S. Kim
Clinical Trial Center, Asan Medical Center
Seoul, Republic of Korea

I.-J. Jang
Department of Clinical Pharmacology and Therapeutics
Seoul National University College of Medicine and Hospital
Seoul, Republic of Korea

the attrition rates. In this process, earlier and more correct characterization of a candidate drug and prediction based on this information of the future under various scenarios are very important, as consequently, many pivotal decisions could be made more reliably in earlier phases. Biomarkers reflecting the mechanism of action of a drug are receiving attention as a key bridge linking these early observations of the drug and the clinical outcomes in later stage of drug development. Application of imaging biomarkers using positron emission tomography (PET) in drug development has been rising rapidly since late 1980's with almost 400 papers from 2010 alone (1,2). PET enables us to test the biodistribution of a new chemical entity to the target tissue in high concentrations enough to be pharmaceutically active, and quantify the relationship between the concentration of a new chemical entity and its interaction with the target of interest. The concentration-receptor occupancy relationship could be much informative in identifying and guiding optimal doses if its association with the pharmacological effect of the new entity is known.

The model-based drug development is a novel paradigm proposed to make the drug development processes efficient, and has been increasingly used (3,4). US FDA and EMEA have been fueling these approaches (5,6) in whole clinical development stages of a drug.

In CNS research which uses the imaging biomarker most actively in drug development process, the term 'proof of mechanism' is frequently used (7). Generally, the term 'proof of mechanism' in new drug development is used when a novel drug candidiate is shown to act following its proposed mechanism in human body. Most often, the proof of mechanism is shown by using mechanism based biomarker, and this tells us that the probability of the existence of drug effect is relatively high. Pharmacokinetic (PK)/pharmacodynamic (PD) mixed effect modeling and Monte-Carlo simulation are also the important methods in drug development, and are widely applied to characterize candidate drugs quantitatively and predict effect and safety outcomes for various scenarios in the drug development process.

Striatal dopamine (D_2) receptor blockade plays a pivotal role in the therapeutic effects of many antipsychotics, including atypical antipsychotics with relatively lower affinity to the D_2 receptor (8). Brain imaging modalities such as PET permit the observation of *in vivo* receptor binding activity in humans. D_2 receptor occupancy is important in that it reflects the mechanism of action of D_2 antagonists in the human body. The positive slope in the relationship between dose and D_2 receptor occupancy can be regarded as strong evidence that a drug acts by its mechanism of action in humans (9). The relationship between D_2 receptor occupancy and the treatment effect or extrapyramidal syndromes (EPS) induced by antipsychotics is well established. For most antipsychotics including haloperidol, a therapeutic window of 65% – 80% or 70% – 80% has been proposed, as occupancy exceeding 80% is associated with EPS, whereas that exceeding 65 or 70% results in a therapeutic effect (10). This information could be used as a guide for finding optimal dosing regimens of newly developed antipsychotics in early stages of the development process, and the dosing regimens could be adopted in later stages of development.

Radiolabeling of drugs with positron-emitting radionuclides of [^{11}C] or [^{11}F] is the most commonly used one in measurement of the engagement of therapeutic targets by drug candidates (7). [^{18}F] fallypride is one of the currently available PET radiotracer that can reliably provide quantitative measures of D_2 receptor binding in both striatum and extrastriatal brain regions in the same scanning session because [^{18}F] fallypride scanning sessions can be extended for a longer duration than for [^{11}C] labeled radioligands (11,12). While [^{11}C] raclopride has fast *in vivo* kinetics and moderate *in vivo* affinity for dopamine D_2 receptors, due to its relatively low signal to noise ratio, it can provide a measure of D_2 receptor availabilty only in the striatum, where the receptor density is high. Although [^{18}F] fallypride has slow kinetics in the striatum, its high affinity and signal-to-noise ratio together with relatively long physical half-life make it possible to reliably measure D_2 receptor availability both in the striatum and extrastriatal regions with lower receptor density (11).

Haloperidol is a prototypical compound of the butyrophenone class that has been widely used in the treatment of schizophrenia, mania, and other psychiatric disorders (13). Haloperidol has a narrow therapeutic window and exhibits large inter-individual PK variation (14). The PK of haloperidol is reported to be affected by many factors in a complex manner (15). Oral haloperidol is absorbed well with absolute bioavailability from 60% to 70%. Average tmax and elimination half-life values showed wide variance among studies from 1.7 to 6.1 h and 14.5 to 36.7 h. Haloperidol is extensively metabolized in liver, and the free fraction in human plasma is 7.5 to 11.6% (16).

The current receptor occupancy study was designed to evaluate the possibility of using D_2 receptor occupancy measurements in humans *via* PET imaging using [^{18}F] fallypride and modeling and simulation analysis in early clinical stages of the antipsychotic drug development process by using haloperidol as a model drug.

METHODS

Subjects

All the enrolled subjects were healthy male Korean volunteers aged 19 to 45 years, who weighed 57.0 to 89.9 kg and were within 20% of ideal body weight (kg) which was calculated as (height in cm − 100) × 0.9. All the subjects were deemed eligible for the study when they met all of the inclusion and exclusion criteria. None of the subjects had

significant cardiac, hepatic, renal, pulmonary, neurologic, gastrointestinal, or hematologic disorders, as determined by medical history, physical examination. None of the subjects had a history of alcohol or drug abuse and none of the subjects had a history of allergic or adverse response to haloperidol or any related drug.

This study was conducted in Seoul National University Bundang Hospital, Seongnam, Republic of Korea, and Asan Medical Center, Seoul, Republic of Korea after approval by institutional review board of each institute. This study was conducted in accordance with the principles of the declaration of Helsinki and revisions and the international conference on harmonization guidance for good clinical practice (ICH GCP). All the subjects gave written informed consent before enrollment. This clinical study is registered on-line at ClinicalTrials.gov (registration number: NCT01193621).

Study Design

This was a multiple dosing, open, parallel, group study. 0.5, 1, or 3 mg of haloperidol was administered orally once a day for 7 days to 3, 2, and 3 subjects in each dose group, respectively (N=8). Alcohol, intense physical activity, and smoking were not allowed during the study. PET for D_2-receptor occupancy was scanned using [^{18}F] fallypride with following schedule based on the beginning time of PET scan for 2 h; Prior to the first haloperidol administration (baseline, day 0), and 24 h (day 8), 120 h (day 12) after the last (7th) haloperidol administration. For PK analysis, blood was scheduled to be drawn (6 ml, each) prior to the haloperidol administration (day 1 0 h), and 6 h (1 day 6 h), 24 h (2 day 0 h), 48 h (3 day 0 h), 96 h (5 day 0 h), 144 h (7 day 0 h) relative to the first drug administration on day 1, and, 0.5, 1, 2, 4, 6, 8, 12, 24 h (8 day 0 h), 48 h (9 day 0 h), 72 h (10 day 0 h), 168 h (14 day) after taking the last oral dose of haloperidol on day 7 (Fig. 1). All the blood samples were centrifuged for 10 min at 1,200 g at 4°C immediately after collection from the study subjects. Plasma samples were transferred to cryovial tubes and stored at −70°C until assay.

Synthesis of [^{18}F] Fallypride

The details of the procedures for synthesis of [^{18}F]fallypride have been reported (17). Briefly, a fully automated synthesis of [^{18}F]fallypride was carried out by fluorine-18 and tosyl-fallypride using our newly developed synthetic method. [^{18}F]Fallypride was obtained with a high radiochemical yield of 68% (decay-corrected) and specific activity of approximately 140-192 GBq/μmol at the time of injection.

PET Scan Procedure

A PET scan with [^{18}F]fallypride (0.1 mCi/kg) bolus injection was performed using PET/CT (computerized tomography) scanners (GE Discovery VCT) in 3-dimensional mode with resolutions of 4.87 mm (radial), 5.84 mm (tangential), and 4.4 mm (axial) at 1 cm offset from the center of the field of view (18).

Two dynamic PET scans were performed for a total of 3 h: first session for 80 min (20 s×3, 1 min×3, 2 min×3, 4 min×5, and 5 min×10) and second session for 70 min (10 min×7). Subjects were permitted to leave the scanner for 30 min between the two sessions. Before each PET scan, low-dose helical CT was obtained for attenuation correction. PET frames were realigned to a first 30 min averaged PET image to generate a motion-corrected dynamic image. 1.5TT1-weighted MRI (magnetic resonance imaging) scans of the brain were obtained at a separate time for the purpose of anatomical co-registration. Region of interests (putamen, caudate, cerebellum) were drawn on MRI. Individual MR (magnetic resonance) image was co-registered to the PET space to extract time-activity curves using PMOD 3.13 software (PMOD Technologies, Zurich, Switzerland).

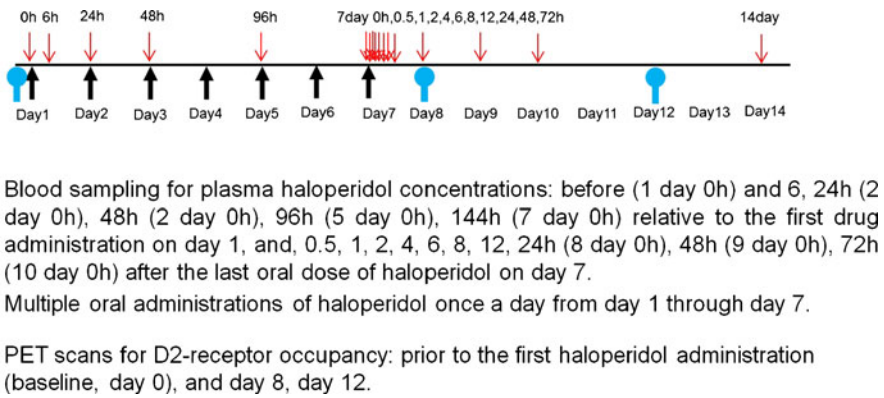

Fig. 1 Overall schedule of the study.

D_2 Receptor Occupancy Measurement

PET outcome measure was binding potential (BP), which is a measure of the capacity of a brain region for specific binding of radioligand and is equivalent to the ratio of B_{max} (density of available binding sites) to K_D (affinity of the radioligand for available binding sites) (19).

BP for each region was calculated using the simplified reference tissue model using cerebellum as a reference region (20). Receptor occupancy after haloperidol treatment was defined as percent reduction of BP relative to the individual baseline BP estimates ($= 100 \times (BP_{Baseline} - BP)/BP_{Baseline}$).

Measurement of Plasma Haloperidol

The plasma haloperidol concentrations were determined using high-performance liquid chromatography (Symbiosis™, Spark Holland Instruments, Emmen, The Netherlands) with tandem mass spectrometry (API 4000; ABSciex, Inc., Foster City, CA) after sample preparation by liquid-liquid extraction (21). In brief, samples were removed from the freezer and allowed to thaw at room temperature (25°C). A total of 200 μl of the thawed plasma sample was mixed with 10 μl internal standard (flecainide, 10 ng/ml) for 10 s. Two milliliters of ethyl ether were added to the mixture and then mixed for 1 min and centrifuged at 3500 g for 15 min. The upper layer was transferred into a culture tube (Pyrex culture tube, 12×75 mm) and evaporated to dryness under a speed vac (45°C, 40 min). The dry residue was reconstituted in 50 μl mobile phase and centrifuged at 16,853 rpm (4°C, 40 min). The upper layer was transferred into auto-injection vial for analysis by liquid chromatography-tandem mass spectrometry (LC-MS-MS). The lower limit of quantification was 0.05 ng/ml. The calibration curve was linear over the range of 0.05~50.0 ng/ml, with the coefficients of determination (R^2) of 0.9986~0.9989. The intra- and inter-assay precision levels were determined for four quality control concentrations of haloperidol, 0.05, 0.2, 2, and 40 ng/ml. The coefficients of variation of the intra- and inter-assay precision were 3.78~19.38% and 1.07~10.39%, respectively. The accuracy values of the intra- and inter-assay were 92.3~114.64%, and 92.07~102.37%, respectively.

Pharmacokinetic and Pharmacodynamic Analysis of Haloperidol

The PK and PD of haloperidol were analyzed with nonlinear mixed effects modeling using NONMEM (version VII. level 2, ICON Development Solutions, Dublin, Ireland) in conjunction with a gfortran compiler. First-order conditional estimation (FOCE) method with interaction was used for the fitting.

Various PK compartment models with or without nonlinear kinetic components were tried to fit the concentration-time data. D_2 receptor BP data in putamen and caudate nucleus, the main action sites of haloperidol, was modeled subsequently using the individual PK parameter estimates from the final PK model. Effect compartment was introduced in the PD model in order to link plasma haloperidol concentration with the D_2 receptor BP change by haloperidol.

Unexplained inter-individual random variability was modeled with a log-normal model as follows.

$$P_i = P_{TV} \cdot e^{\eta_i}$$

where P_i is the parameter value of the ith individual, P_{TV} is the typical population value for fixed effect parameter, and η is a random variable with a mean of 0 and a variance of ω^2. Inter-individual random variability is represented as ω^2, the variance of η in the log domain.

Model evaluation and selection were based on both graphical and statistical methods. Together with basic goodness of fit plot, predictive checks were performed by simulating 1,000 replications and then comparing the simulated prediction intervals with the original data. R (version 2.14.1; R Foundation for Statistical Computing, Vienna, Austria) software was used for the graphical model diagnosis. Log likelihood ratio test was used to discriminate between hierarchical models. A P-value of 0.05, representing a decrease in objective function value (OFV) of 3.84 points, was considered statistically significant (chi-square distribution, degree of freedom=1, which was applied to all the parameters in the model including fixed effect parameters and those for inter-individual variations of the fixed effect parameters.

Monte-Carlo Simulation for D_2 Receptor Occupancy

To investigate the relationship between steady state plasma concentration of haloperidol and D_2 receptor occupancy, Monte-Carlo simulation was conducted using the PD model for BP. Size of unexplained inter-individual variability, and residual error of the model output were used as source of variability for the simulation under the assumption of normal distribution with 0 mean. The simulation result is displayed in Fig. 5, together with 90% prediction intervals for steady state plasma concentration on haloperidol 1 mg or 3 mg, every 24 h.

Another Monte-Carlo simulation was conducted in order to investigate the optimal dosing regimen of haloperidol by predicting the D_2 receptor occupancy changes over time on various dosing regimens of haloperidol (0.5, 1, 2, or 3 mg every 12 h or 24 h) using

Table I D_2 Receptor Occupancy on 24 h† After the 7th Dosing of Once a Day Administration of Haloperidol by Doses

Organ	Dose (mg)	AUC_{7day} (ng*h/ml)	D2RO (%)	No. of subjects
Putamen	0.5	5.6 (38.6)	15.1 (49.1)	3
	1	16.5 (14.9)	35.7 (30.0)	2
	3	55.1 (20.8)	46.3 (27.4)	3
Caudate Nucleus	0.5	5.6 (38.6)	17.3 (39.9)	3
	1	16.5 (14.9)	39.6 (31.7)	2
	3	55.1 (20.8)	52.4 (25.6)	3

Mean (coefficient of variation in %) values are presented

AUC_{7day} Interval area under the concentration time curve from day 7 0 h through day 8 0 h; *D2RO* D_2 receptor occupancy; *SD* standard deviation

† 24 h is scheduled time, and actual times of the PET measurement are not exactly same with the scheduled time

the final PK and PD models built in this study. In this simulation, size of unexplained inter-individual variability, and residual error of the PD model output were used as source of random variables for the simulation under the assumption of normal distribution with mean of zero.

All the simulation was conducted using NONMEM, and D_2 receptor occupancy (%) at each time point was calculated from simulated BP values as following equation.

$$RO(\%) = 100 \times (E0 - BP)/E0$$

where RO is D_2 receptor occupancy, BP is simulated BP, and $E0$ is the baseline BP of each subject.

RESULTS

The average, observed D_2 receptor occupancies (%), and 24-hour interval area under the concentration time curve on day 7 after the 7th haloperidol administration of the multiple once a day were shown by each dose in Table I. D_2 receptor occupancies by haloperidol increased by the doses administered.

Pharmacokinetics of Haloperidol

The plasma concentration of haloperidol was best described by a one-compartment model with a saturable binding compartment, a sequential zero- and first-order absorption

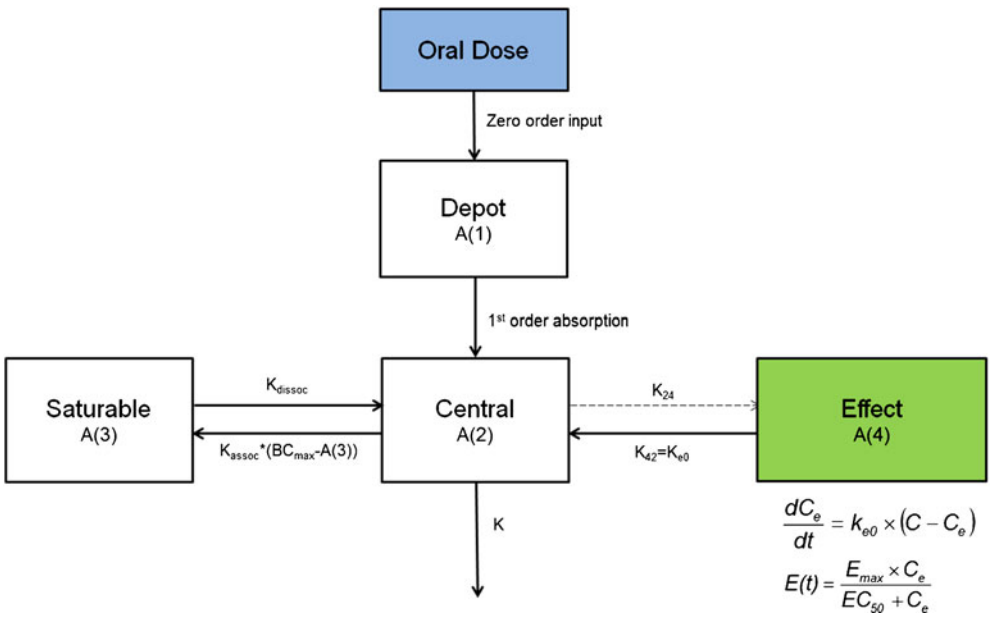

Fig. 2 Diagram for pharmacokinetic-pharmacodynamic model in this study. Abbreviations: *k*, elimination rate constant; k_{assoc}, association constant; k_{dissoc}, dissociation constants for haloperidol and receptor binding; BC_{max}, maximum binding capacity; *A(1)*, haloperidol amount in Depot compartment; *A(2)*, haloperidol amount in central compartment; *A(3)*, haloperidol amount in the binding compartment; *A(4)*, haloperidol amount in effect compartment; Negligible amount of drugs enter the effect compartment (small k_{24}); The rate of equilibration is determined by k_{e0}; C_e, haloperidol concentration in effect compartment; E(t), effect at time t; E_{max}, maximal effect; EC_{50}, C_e at half-maximal effect.

with time lag in the beginning of absorption, and a proportional error (Fig. 2). A linear one- or two-compartment model with oral absorption did not predict the high concentrations of haloperidol around peak plasma concentrations well, as severe under-predictions were observed. The addition of a compartment in the model, the transfer to which is described to be saturable, significantly improved the fit (-546.510 *versus* -694.132 in OFV), and corrected the under-prediction of the higher concentrations substantially as follows:

$$K_{23} = K_{assoc} * (BC_{\max} - A(3))$$
$$K_{32} = K_{dissoc}$$

where k_{23} and k_{32} are the rate constants from the central compartment to the binding compartment and from the binding compartment to the central compartment, respectively, k_{assoc} and k_{dissoc} are the association and dissociation constants for haloperidol and receptor binding, respectively, BC_{max} is the maximum binding capacity in a binding compartment, and $A(3)$ is the amount of haloperidol in the binding compartment.

PK data were analyzed using the NONMEM subroutine ADVAN6. Observed plasma concentrations *versus* model-predicted concentrations over time and the predictive check plots by doses reveal that the PK model predicts the observed concentrations well (Fig. 3). The predictive check plots of the model are also shown in Fig. 3. η-Shrinkage was less than 14.1%, and ε-shrinkage was 10%. Estimates of the fixed effect PK parameters and the size of the unexplained inter-individual variability of some fixed effect parameters are summarized in Table II.

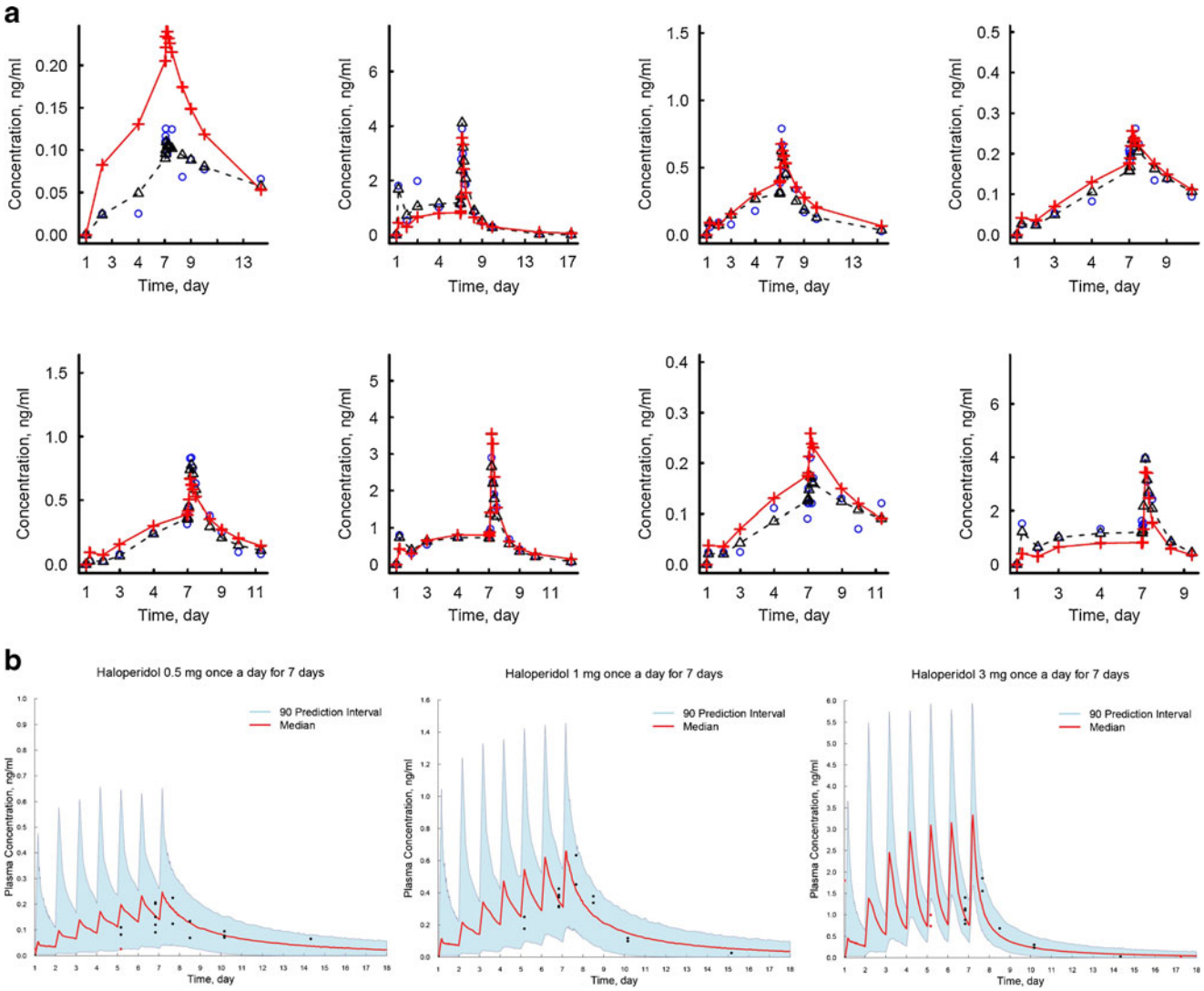

Fig. 3 Observed plasma haloperidol concentrations *versus* model-predicted haloperidol concentrations and visual predictive check plots for the haloperidol pharmacokinetic model. †Empty blue circles are the observed haloperidol concentrations. Red solid lines and crosses are the population predictions of haloperidol concentrations. Black dashed lines and triangles are the individual predictions of haloperidol concentrations. ††Solid circles are the observed haloperidol concentrations.

Table II Pharmacokinetic Parameter Estimates for Multiple Haloperidol Dosing in Eight Healthy Male Subjects

Parameter	Estimate	RSE (%)	95% CI
Ka, 1/h	1.17	9.1	0.96～1.38
D1, h	3.08	58.1	-0.08～1.26
ALAG1, h	0.866	11.0	0.679～1.053
Vc/F, L	153	43.6	22～284
$IIV_{Vc/F}$ (CV %)	1.75 (218.1)	36.9	0.49～3.01
BC_{max}, mg	6.18	20.7	3.67～8.69
IIV_{Bmax} (CV %)	0.146 (49.2)	49.2	0.005～0.287
K_{assoc},/h	5.79	12.1	4.42～7.16
K_{dissoc},/h	0.431	8.3	0.361～0.501
CL/F, L/h	75	8.7	62～88
$IIV_{CL/F}$ (CV %)	0.0353 (19.0)	32.3	0.0130～0.0576
ε (proportional)	0.235[†]	20.9	0.087～0.209

RSE relative standard error (standard error divided by the parameter estimate); *IIV* inter-individual variability; *Ka* absorption rate constant; *D1* duration of zero-order absorption; *ALAG1* absorption lag time; V_d/F central volume of distribution divided by bioavailability; BC_{max} maximum binding capacity in a binding compartment; K_{assoc} association rate constant; K_{dissoc} dissociation rate constant; *CL/F* clearance divided by bioavailability; *F* bioavailability

[†] ε (proportional) represents the coefficient of variation

Pharmacokinetic–Pharmacodynamic Analysis of Haloperidol

A simple inhibitory E_{max} model in the effect compartment with an additive residual error model was the best model for the relationship between plasma haloperidol concentrations and D_2 receptor BP in both the putamen and caudate nucleus. The parameter for the unexplained inter-individual variability of the fixed effect parameter was allowed only for the baseline BP in this dataset. The plasma haloperidol concentrations at half-maximal inhibition of D_2 receptor binding were 0.791 ng/ml in the putamen and 0.650 ng/ml in the caudate nucleus. The distributional half-lives of the effect compartment, which reflects the temporal dissociation (hysteresis) between the plasma concentration of haloperidol and D_2 receptor binding, as calculated from ke0 (elimination rate constant from the effect compartment to the central compartment) were 3.25 and 3.32 h in the putamen and caudate nucleus, respectively. The analysis results are summarized in Table III.

Predictive check plots for D_2 BP and D_2 receptor occupancy, which was calculated from the BP, are shown in Fig. 4. η-Shrinkage and ε-shrinkage were 16.2% and 10.8% for the putamen and 7.0% and 13.5% for the caudate nucleus, respectively.

Monte-Carlo Simulation for the D_2 Receptor Occupancy on Haloperidol

The predicted relationship between D_2 receptor occupancy and steady-state plasma concentrations in the range of 0–5 ng/ml, which encompasses the once-daily administration of 1 or 3 mg of haloperidol, is displayed in Fig. 5. This result reveals a clear increment of D_2 receptor occupancy with increasing haloperidol doses in the range of 0.5–3 mg in both the putamen and caudate nucleus. The plots of the

Table III Pharmacodynamic Parameter Estimates for the Relationship Between Plasma Haloperidol Concentrations and D_2 Binding Potential for Multiple Haloperidol Dosing in Eight Healthy Male Subjects

Organ	Parameter	Estimate	RSE (%)	95% CI
PUTAMEN	E_0	26.9	3.0	25.3-28.5
	IIV_{E0} (CV %)	0.00341 (5.84)	55.4	-0.00029-0.00711
	C_{50}, ng/mL	0.791	11.9	0.606-0.976
	GAM	1	-	-
	K_{e0}, 1/h	0.213	13.5	0.157-0.269
	ε (additive)	1.86 [a]	10.4	1.48-2.24
CAUDATE	E_0	22.9	3.9	21.2-24.6
	IIV_{E0} (CV %)	0.00693 (8.33)	70.9	-0.00269-0.01655
	C_{50}, ng/mL	0.650	11.6	0.502-0.798
	GAM	1	-	-
	K_{e0}, 1/h	0.209	0.9	0.205-0.213
	ε (additive)	0.159 [†]	9.5	1.29-1.89

RSE relative standard error (standard error divided by the parameter estimate); *IIV* inter-individual variability; E_0 baseline binding potential; C_{50} concentration at half-maximal inhibition; *GAM* Hill coefficient, fixed to 1; K_{e0} elimination rate constant from effect compartment to central compartment

[†] ε (additive) represents the standard deviation

Monte-Carlo simulation for the changes in D_2 receptor occupancy over time using the PK/PD model for various dosing regimens of haloperidol facilitated the selection of the optimal dosing regimens by comparing the median and prediction interval with the suggested therapeutic target range of D_2 receptor occupancy (10). Example plots for the changes of D_2 receptor occupancy over time together with corresponding plasma concentrations for various dosing regimens of haloperidol predicted by the PK-PD model are shown in Fig. 6. As an example, the median and 90% prediction interval for the D_2 receptor occupancy of haloperidol 3 mg every 24 h or 2 mg every 12 h were demonstrated to be similar to the therapeutic target window of D_2 receptor occupancy.

DISCUSSION

In this study, a PET scan was conducted only three times in each subject. After baseline PET scan, PET scan was conducted on day 8 after multiple dosing until day 7, where we assumed steady state PD; that is, an equilibrium in average amount of haloperidol across putamen, or caudate nucleus in the brain and the plasma already had been reached on day 8. Thus, we expected to observe more clear differences in D_2 BP, hence D_2 receptor occupancy among the dose groups of haloperidol even with sparse PET scans per subject. Another PET scan was performed around day 12, which together with that on day 8 potentially provides kinetic information on the temporal displacement between plasma *versus* time and D_2 receptor occupancy *versus* time, probably due to the distributional non-equilibrium of haloperidol across the putamen or caudate nucleus in the brain and the plasma. The temporal displacement was reflected in the estimates for the distributional half-lives in the effect compartments in the PK-PD model, and the distributional half-lives were similar between the putamen and the caudate nucleus at 3.25 and 3.32 h, respectively. We can estimate the onset of action of the drug from the half-life, which could be useful in the treatment of psychosis.

The PK of haloperidol was not described by conventional linear compartmental models. There was severe under-prediction during absorption phase, early after the drug administration. Although we increased the PK compartments for the drug distribution, the under-prediction has not been improved at all. Since we measure the plasma drug concentration, if a drug has significant limitation in distribution to peripheral tissues, either saturable binding or saturable transport, much higher plasma concentrations than those predicted by linear distributional PK model would be observed around maximum plasma concentrations, earlier than disposition phase. Paclitaxel is one example that shows the saturable distribution to tissues (22).

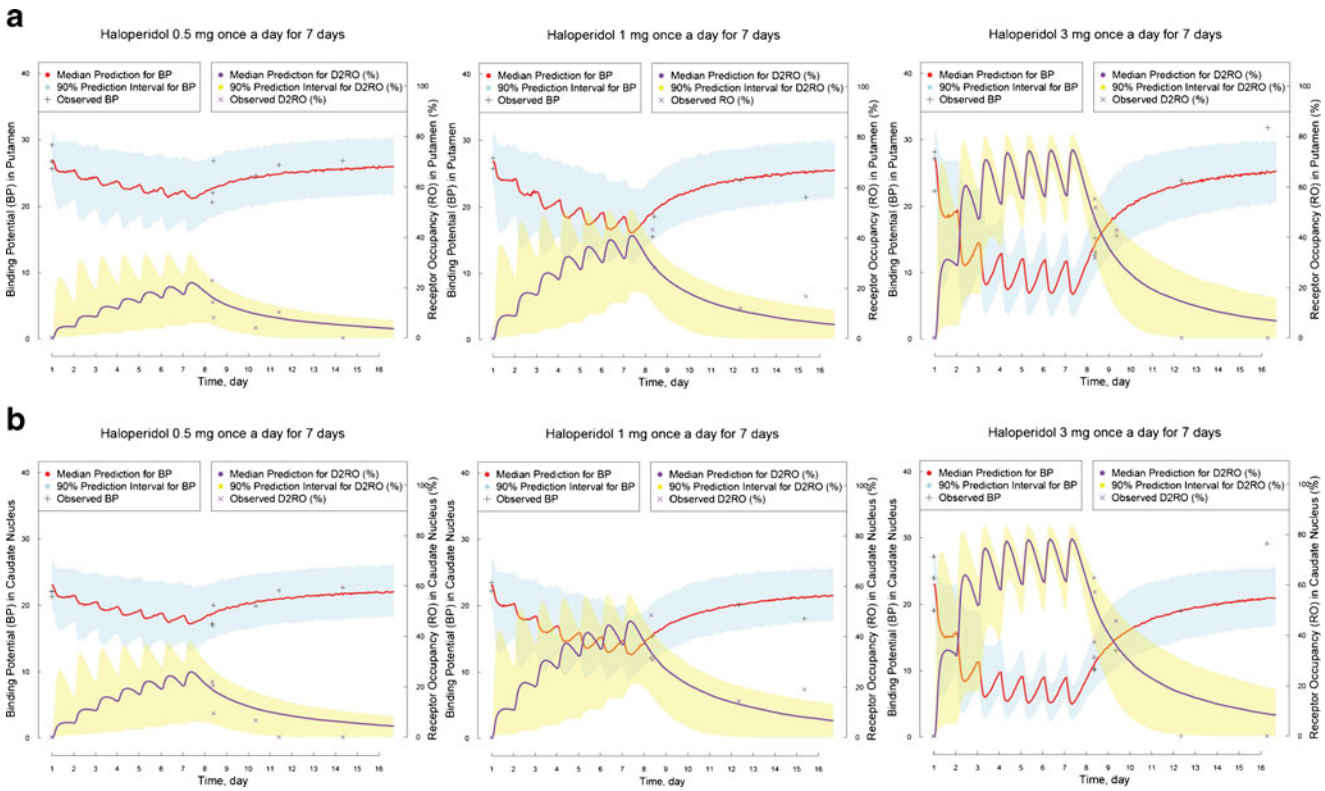

Fig. 4 Visual predictive check plots for the haloperidol pharmacokinetic-pharmacodynamic (D_2 binding potential and D_2 receptor occupancy) models.

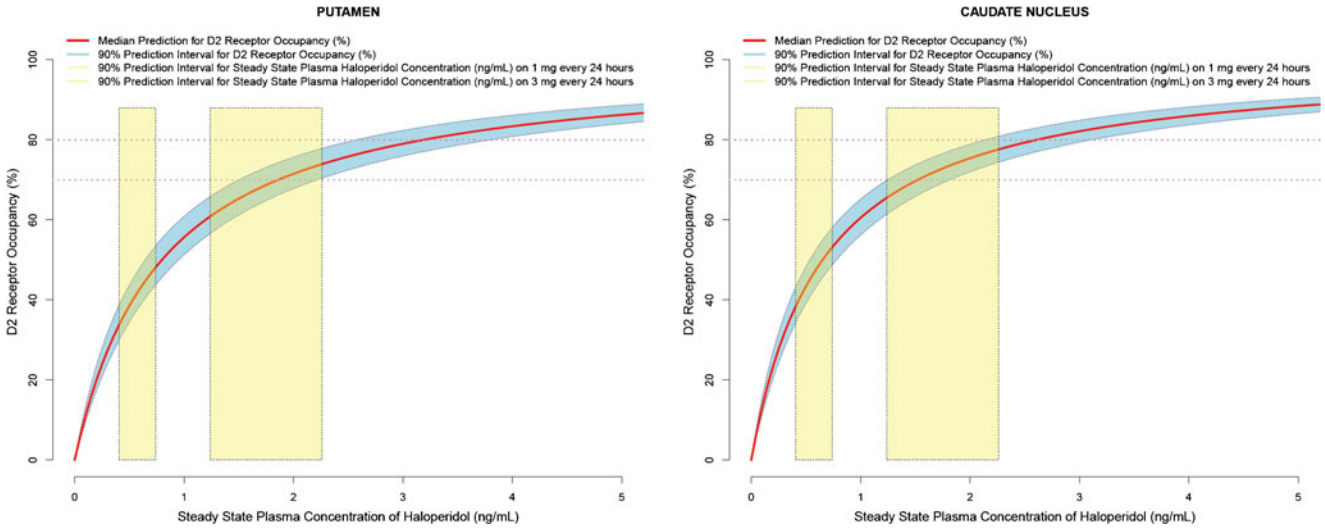

Fig. 5 Relationship between model-predicted D_2 receptor occupancy and steady-state plasma haloperidol concentration. †Monte-Carlo simulation for the relationship between concentration and D_2 receptor occupancy was performed using the size of the unexplained inter-individual variability, standard errors of fixed effect parameter estimates, and residual error from the E_{max} model in this study as the sources of variability under the assumption of normal distribution with a mean of zero. ††90% prediction interval for the steady-state plasma concentration of haloperidol was obtained from the Monte-Carlo simulation using the unexplained inter-individual variability and residual error as the sources of variability under the assumption of normal distribution with mean of zero.

Although the final PK-PD model predicted the observed values reasonably well in Fig. 4, there is a little under-prediction in the D2RO. We tried other, more flexible models with more parameters including sigmoid Emax model, rather than simple Emax model, but the models were not successful with our data.

In Fig. 5, model-predicted D_2 receptor occupancy increased as the plasma concentration of haloperidol increased. This dose dependent D_2 receptor occupancy relationship could be regarded as strong evidence that D_2 antagonist exerts its effects according to its mechanism in human *in vivo* (8). This information could provide us the possibility of the treatment effect of a novel D_2 antagonist under development in earlier phases, which would be useful in making early go/no go decision. It was reported that D_2 receptor occupancy exceeding 65% or 70% was sufficient for an antipsychotic effect, whereas occupancy exceeding 80% was associated with an increased risk of EPS (9,23), which applies to most of the second-generation, 'atypical' antipsychotics, although there are some exceptions such as

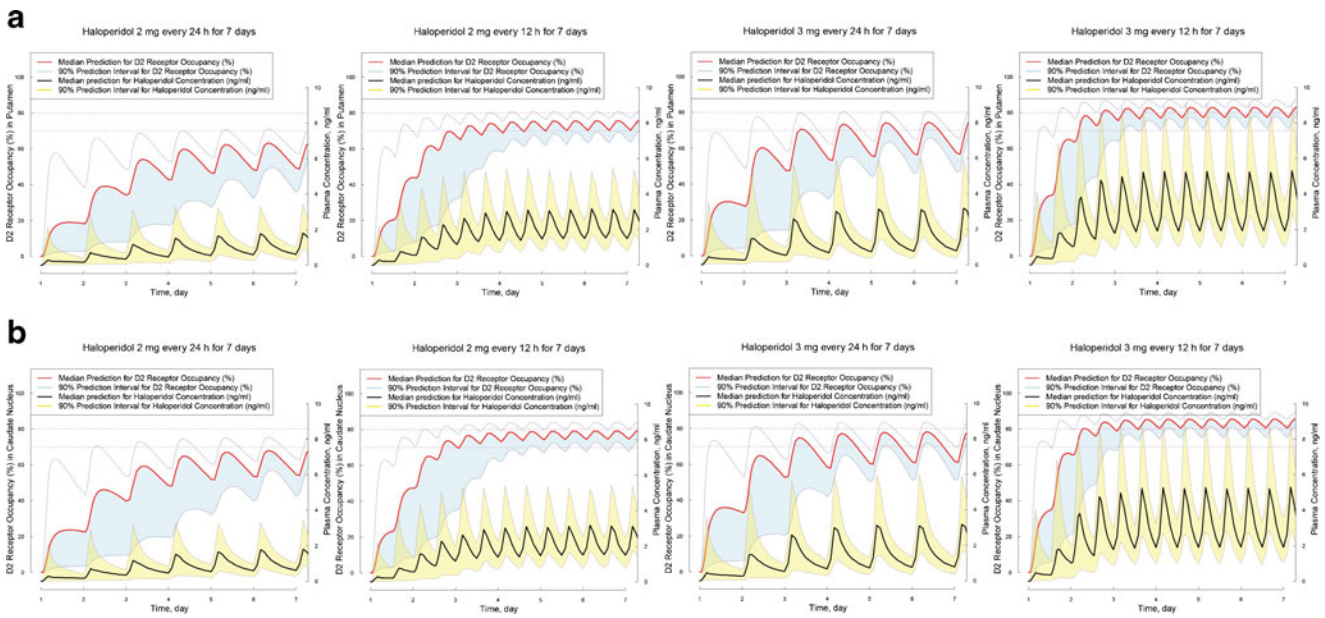

Fig. 6 Monte-Carlo simulation for plasma concentration and D_2 receptor occupancy for various dosing regimens of haloperidol.

aripiprazole, which induces no EPS even at striatal D_2 receptor occupancy values exceeding 90% (24–26). This therapeutic window may be useful in finding the dosing regimens of D_2 antagonists for optimal treatment. The relationship between doses of antipsychotics and their striatal D2 receptor occupancy has proven to be biomarker, critical in decision making in the development of new psychotropic drugs (27). As shown in Fig. 6, using the PK/PD model built in this study, D_2 receptor occupancy changes over time could be simulated for various dosing regimens by considering the unexplained inter-individual variation in a population and residual variability of the model. In the examples of Fig. 6, haloperidol 2 mg every 12 h appears to be an optimal dosing regimen when we compare the occupancy window and predicted D_2 receptor occupancy using both the median values and the 90% prediction interval. For 24-hour interval regimens, the difference between maximum and minimum occupancy is predicted to be large, resulting in occupancy outside the target window for a longer time at 24-hour dosing interval than 12-hour interval. However, it is not known whether the size of the fluctuation in D_2 occupancy affects the treatment outcome or whether the average D_2 occupancy during multiple administrations of a D_2 antagonist is more important. This issue should be elucidated in future research. This simulation results are consistent with the previously reported optimally effective haloperidol doses of 50–100 mg every 4 weeks (28).

CONCLUSION

In this clinical study, we clearly demonstrated that haloperidol acts according to its proposed mechanism of action by observing the increment of D_2 receptor occupancy with increasing doses of haloperidol in the range of 0.5–3 mg with relative sparse PET imaging data (three scans per subject). Referencing the suggested D_2 receptor occupancy window of 65 or 70% to 80% for the optimal therapeutic outcome of D_2 antagonists, we showed that the optimal dosing regimens of haloperidol could be suggested *via* extensive Monte-Carlo simulations. The doses identified in this way correspond to the currently recommended therapeutic dosing regimens of haloperidol. The methodology applied in this study of the combined use of D_2 receptor occupancy and modeling/simulation may be applied in earlier stages of the development of novel D_2 receptor antagonists in healthy subjects, making the development process more efficient with reduced attrition rates.

ACKNOWLEDGMENTS AND DISCLOSURES

This study was supported by a grant of the Korea Healthcare Technology R&D Project, Ministry for Health & Welfare, Republic of Korea.(A102158 and A070001). The authors declare they have no conflict of interest.

REFERENCES

1. Matthews PM, Rabiner EA, Passchier J, Gunn RN. Positron emission tomography molecular imaging for drug development. Br J Clin Pharmacol. 2012;73:175–86.
2. Bergström M, Grahnén A, Långström B. Positron emission tomography microdosing: a new concept with application in tracer and early clinical drug development. Eur J Clin Pharmacol. 2003;59:357–66.
3. Nucci G, Gomeni R, Poggesi I. Model-based approaches to increase efficiency of drug development in schizophrenia: a can't miss opportunity. Expert Opin Drug Discov. 2009;4:837–56.
4. Holford N, Ma SC, Ploeger BA. Clinical trial simulation: a review. Clin Pharmacol Ther. 2010;88:166–82.
5. Available from: http://www.fda.gov/ScienceResearch/SpecialTopics/CriticalPathInitiative/CriticalPathOpportunitiesReports/ucm077262.htm Critical Path initiative. [Accessed 17 July 2012]
6. Available from: http://www.ema.europa.eu/docs/en_GB/document_library/Report/2011/01/WC500101373.pdf. The European Medicines Agency Road Map to 2015: The European Medicines Agency's contribution to science, medicines and health. [Accessed 17 July 2012]
7. Wong DF, Tauscher J, Gründer G. The role of imaging in proof of concept for CNS drug discovery and development. Neuropsychopharmacology. 2009;34:187–203.
8. Kapur S, Remington G. Dopamine D(2) receptors and their role in atypical antipsychotic action: still necessary and may even be sufficient. Biol Psychiatry. 2001;50:873–83.
9. ICH. ICH Topic E4: Dose-response information to support drug registration. 1994.
10. Farde L, Nordström AL, Wiesel FA, Pauli S, Halldin C, Sedvall G. Positron emission tomographic analysis of central D1 and D2 dopamine receptor occupancy in patients treated with classical neuroleptics and clozapine. Relation to extrapyramidal side effects. Arch Gen Psychiatry. 1992;49:538–44.
11. Slifstein M, Kegeles LS, Xu X, Thompson JL, Urban N, Castrillon J, Hackett E, Bae SA, Laruelle M, Abi-Dargham A. Striatal and extrastriatal dopamine release measured with PET and [(18)F] fallypride. Synapse. 2010;64:350–62.
12. Kessler RM, Ansari MS, Riccardi P, Li R, Jayathilake K, Dawant B, Meltzer HY. Occupancy of striatal and extrastriatal dopamine D2/D3 receptors by olanzapine and haloperidol. Neuropsychopharmacology. 2005;30:2283–9.
13. Mutschler E, Derendorf H. Drug actions; basic principles and therapeutic aspects. Stuttgart: Medpharm Scientific Publishers; 1995.
14. Ulrich S, Wurthmann C, Brosz M, Meyer FP. The relationship between serum concentration and therapeutic effect of haloperidol in patients with acute schizophrenia. Clin Pharmacokinet. 1998;34:227–63.
15. Yukawa E, Hokazono T, Yukawa M, Ichimaru R, Maki T, Matsunaga K, Ohdo S, Anai M, Higuchi S, Goto Y. Population pharmacokinetics of haloperidol using routine clinical pharmacokinetic data in Japanese patients. Clin Pharmacokinet. 2002;41:153–9.
16. Kudo S, Ishizaki T. Pharmacokinetics of haloperidol: an update. Clin Pharmacokinet. 1999;37:435–56.
17. Moon BS, Park JH, Lee HJ, Kim JS, Kil HS, Lee BS, Chi DY, Byung Chul Lee Y, Kim K, Kim SE. Highly efficient production of [^{18}F]Fallypride with fully automated synthesis system. Appl Radiat Isot. 2010;68:2279–84.
18. Teras M, Tolvanen T, Johansson JJ, Williams JJ, Knuuti J. Performance of the new generation of whole-body PET/CT scanners: Discovery STE and Discovery VCT. Eur J Nucl Med Mol Imaging. 2007;34:1683–92.
19. Innis RB, Cunningham VJ, Delforge J, Fujita M, Gjedde A, Gunn RN, Holden J, Houle S, Huang SC, Ichise M, Iida H, Ito H, Kimura

Y, Koeppe RA, Knudsen GM, Knuuti J, Lammertsma AA, Laruelle M, Logan J, Maguire RP, Mintun MA, Morris ED, Parsey R, Price JC, Slifstein M, Sossi V, Suhara T, Votaw JR, Wong DF, Carson RE. Consensus nomenclature for *in vivo* imaging of reversibly binding radioligands. J Cereb Blood Flow Metab. 2007;27:1533–9.
20. Lammertsma AA, Hume SP. Simplified reference tissue model for PET receptor studies. NeuroImage. 1996;4:153–8.
21. Zhang G, Terry Jr AV, Bartlett MG. Liquid chromatography/tandem mass spectrometry method for the simultaneous determination of olanzapine, risperidone, 9-hydroxyrisperidone, clozapine, haloperidol and ziprasidone in rat plasma. Rapid Commun Mass Spectrom. 2007;21:920–8.
22. Karlsson MO, Molnar V, Freijs A, Nygren P, Bergh J, Larsson R. Pharmacokinetic models for the saturable distribution of paclitaxel. Drug Metab Dispos. 1999;27:1220–3.
23. Kapur S, Zipursky R, Jones C, Remington G, Houle S. Relationship between dopamine D(2) occupancy, clinical response, and side effects: a double-blind PET study of first-episode schizophrenia. Am J Psychiatry. 2000;157:514–20.
24. Nyberg S, Eriksson B, Oxenstierna G, Halldin C, Farde L. Suggested minimal effective dose of risperidone based on PET-measured D2 and 5-HT2A receptor occupancy in schizophrenic patients. Am J Psychiatry. 1999;156:869–75.
25. Nordström A-L, Farde L, Nyberg S, Karlsson P, Halldin C, Sedvall G. D1, D2, and 5-HT2 receptor occupancy in relation to clozapine serum concentration: a PET study of schizophrenic patients. Am J Psychiatry. 1995;152:1444–9.
26. Yokoi F, Gründer G, Biziere K, Stephane M, Dogan AS, Dannals RF, Ravert H, Suri A, Bramer S, Wong DF. Dopamine D2 and D3 receptor occupancy in normal humans treated with the antipsychotic drug aripiprazole (OPC 14597): a study using positron emission tomography and [11C]raclopride. Neuropsychopharmacology. 2002;27:248–59.
27. Wong DF, Potter WZ, Brasic J. Proof of concept: functional models for drug development in humans. Baltimore, MD: Lippincott Williams & Wilkins; 2002.
28. Taylor D. Establishing a dose-response relationship for haloperidol decanoate. Psychiatrist. 2005;29:104–7.